NACA RM A58A31

NACA

RESEARCH MEMORANDUM

THE EFFECT OF MOMENT-OF-AREA-RULE MODIFICATIONS ON THE ZERO-LIFT DRAG OF THREE WING-BODY COMBINATIONS

By Robert R. Dickey

Ames Aeronautical Laboratory
Moffett Field, Calif.

NATIONAL ADVISORY COMMITTEE
FOR AERONAUTICS

WASHINGTON

May 2, 1958

NACA RM A58A31

NATIONAL ADVISORY COMMITTEE FOR AERONAUTICS

RESEARCH MEMORANDUM

THE EFFECT OF MOMENT-OF-AREA-RULE MODIFICATIONS ON THE ZERO-LIFT DRAG OF THREE WING-BODY COMBINATIONS

By Robert R. Dickey

SUMMARY

An experimental investigation was made to determine the effect on drag of applying the moment-of-area-rule modifications described in NACA RM A54J19 to wing-body combinations with various wing plan forms. The effect of mounting air-to-air type missiles on the wing-mounted bodies of revolution which are part of the moment-of-area-rule modification was also investigated. Wing-body combinations with unswept, sweptback, and triangular plan-form wings having an aspect ratio of 3 and a thickness ratio of 0.03 were employed in the investigation. The zero-lift drag of the moment-of-area-rule configurations was measured and compared with the drag of the corresponding basic wing-body combinations at Mach numbers from 0.6 to 1.4.

At transonic speeds, the moment-of-area-rule modifications provided reductions in the total drag as well as the wave drag for all three wing-body combinations. Although the actual amount of drag reduction was greater for the unswept configuration than it was for the sweptback and triangular configurations, on a percentage basis all three plan forms had approximately 15-percent-less total drag at a Mach number of 1.0 than the corresponding unmodified configuration. At the higher supersonic Mach numbers, the moment-of-area-rule modifications resulted in wave-drag increases for all three wings. Because of the additional surface area of the auxiliary bodies, the modifications also resulted in increases in skin-friction drag.

The method of carrying missiles by mounting them on the moment-of-area-rule pods provided substantial drag reductions when compared to conventional under-the-wing installations. The drag resulting from mounting the four air-to-air type missiles on the pods was in most cases less than the drag of four isolated missiles; whereas, for the conventional installation, the drag due to the addition of the missiles was approximately twice that of four isolated missiles.

INTRODUCTION

A method for reducing the wave drag of wing-body combinations which not only gives low drag at sonic speed but also extends the region of low drag to higher Mach numbers was introduced in reference 1. This method which is called the "moment-of-area rule" differs from the "transonic area rule" (ref. 2) in that, in addition to the longitudinal distribution of cross-sectional area, it also considers the distribution of the moments of area taken about the vertical plane of symmetry. The optimum distributions of the moments of area for a wing-body configuration are obtained by adding auxiliary bodies of revolution to the wing. For low wave drag near a Mach number of 1.0, these wing-mounted bodies or pods are contoured and positioned in such a way that the second moment of area or the moment of inertia about the vertical plane of symmetry of the combined wing and pods has a smooth distribution of high fineness ratio. The optimum distribution of area is obtained by indenting the body to compensate for the cross-sectional areas of the pods as well as the wings so that the resultant total distribution of area is smooth.

Available experimental data on the results of applying the moment-of-area rule to wing-body combinations have thus far been limited to those published in references 1, 3, and 4. Reference 1 shows that large reductions in wave drag were obtained at transonic speeds by modifying an aspect-ratio-2 elliptic plan-form wing and body combination according to the moment-of-area rule. Reference 3 shows that missile installation drags can be reduced by moment-of-area-rule modifications that consider the missiles as part of the wing pods even when such modifications increase the total volume of the configuration. Although the moment-of-area rule was not applied in designing the aspect-ratio-3 straight-wing configurations of reference 4, it was used to explain the relative drag rises of two models designed to have the same average area distribution at Mach number 1.41. The configuration with the better distribution of the second moment of area (model with contoured nacelles) had lower wave drag at all Mach numbers.

The primary purpose of the present investigation was to determine the drag reductions that could be obtained by applying the moment-of-area rule (without changing the total volume) to wing-body combinations having wing plan forms that are typical of current design practice. The moment-of-area-rule configurations were designed to have optimum area and second-moment-of-area distributions for low wave drag near a Mach number of 1.0. A secondary objective was to investigate the use of the moment-of-area-rule pods as supports for carrying missiles when the missiles are not considered to be part of the moment-of-area-rule design and therefore cause deviations from the optimum transonic area distribution. Identical missiles and plan forms were tested in reference 3 with moment-of-area-rule modifications that did include the missiles in the design. However, in the case of reference 3, smooth distributions of area were obtained by adding volume to the sides of the models in the form of localized gloves.

[redacted]

The zero-lift drag of wing-body and wing-body-missile combinations was measured for configurations with unswept, sweptback, and triangular plan-form wings at Mach numbers from 0.6 to 1.4. A constant Reynolds number of 1.5 million based on the mean aerodynamic chords of the wings was maintained throughout the Mach number range.

NOTATION

A	aspect ratio
C_D	foredrag coefficient based on wing area
C_{D_f}	friction-drag coefficient
C_{D_w}	wave-drag coefficient, $C_D - C_{D_f}$
ΔC_{D_w}	incremental wave-drag coefficient, C_{D_w} of total configuration minus C_{D_w} of basic body alone
$\Delta C_{D_{missiles}}$	additional wave-drag coefficient due to missiles, C_{D_w} of total configuration with four missiles minus C_{D_w} of total configuration
l	length of wing pods
M	Mach number
$M_2(0)$	maximum value of second moment of area
$M_2(x)$	longitudinal distribution of the second moment of area
x	longitudinal distance measured from midpoint of wing pod
β	speed parameter, $\sqrt{M^2 - 1}$
τ	maximum thickness ratio of wing

APPARATUS

Models

The basic wing-body combinations were comprised of a cut-off Sears-Haack body and an aspect-ratio-3 wing with either an unswept, a sweptback, or a triangular plan form. The unswept wing had 64A003 airfoil sections, whereas the sweptback and triangular wings had NACA 0003 airfoil

[redacted]

sections. Modified versions of the three basic configurations were obtained by adding pods to the wings and contouring the bodies in accordance with the moment-of-area rule of reference 1. The same total volume was maintained for both the basic and modified configurations. The general arrangement and pertinent dimensions of the three basic configurations and the moment-of-area-rule modifications are shown in figure 1. Tables I and II give the coordinates of the bodies and pods, respectively.

The distributions of area and second moment of area for the basic and modified models are shown in figure 2. Note that the bodies of the moment-of-area-rule models before indentation were slightly larger in diameter than the basic body. The second moment of area of the body is small compared to that of the wing and therefore has been neglected. It may be seen that the additions of the wing pods had the effect of greatly increasing the fineness ratio of the second-moment-of-area distributions.

For the moment-of-area-rule configurations of this investigation, the wing pods were shapes such that the second moment of area of the wing plus pods had a Sears-Haack body (minimum-drag body for given volume and length) type of distribution, as in reference 3; that is,

$$M_2(x) = M_2(0)\left[1 - \left(\frac{x}{l/2}\right)^2\right]^{3/2}$$

This differs from the distribution that was used in reference 1 where

$$M_2(x) = M_2(0)\left[1 - \left(\frac{x}{l/2}\right)^2\right]^{7/2}$$

The Sears-Haack type of distribution results in a low-drag pod with a more practical nose shape which is not cusped.

For the investigation of the use of the moment-of-area-rule pods as supports for missiles, four models of a typical air-to-air type missile were mounted on the pods as shown in figure 3. The addition of the missiles caused the distributions of area and second moment of area to deviate from their previously optimum (for transonic speeds) shapes as may be seen in figure 4.

Wind Tunnel and Equipment

The models were tested in the Ames 2- by 2-foot transonic wind tunnel. This tunnel is of the closed-circuit, variable-pressure type and is equipped with a flexible nozzle and ventilated test section which permits continuous choke-free operation from 0 to 1.4 Mach number. A

complete description of this wind tunnel may be found in reference 5. The forces acting on the models were measured by means of a flexure-type, strain-gage balance which was mounted within the bodies of the models. The models were supported in the wind tunnel by a 1-inch-diameter sting support.

TESTS AND CORRECTIONS

The drag of the various models was measured at zero angle of attack for Mach numbers from 0.6 to 1.4. A constant Reynolds number of 1.5 million based on the mean aerodynamic chords of the wings was maintained throughout the Mach number range by varying the tunnel stagnation pressure. In order to obtain a turbulent boundary layer over the entire surface of the models and thus permit the evaluation of friction drag with a minimum degree of uncertainty, carborundum strips (mean grit height approximately 0.001 inch) were placed near the leading edges of the wings and on the noses of the bodies. The additional wave drag caused by the carborundum strips is believed to be small and should not affect the relative drag levels of the various configurations.

No corrections have been applied to the data for wall-interference effects since reference 5 indicates that for the size of models employed during the present investigation (blockage ratios of approximately 0.5 percent) the effects would be small. Corrections for air-stream angularity and longitudinal pressure gradient were also small and have been neglected. The measured drag of all models was adjusted to correspond to a condition of free-stream static pressure acting at the blunt base of the bodies; therefore, the drag coefficients presented in this report represent the foredrag of the models.

In addition to the small systematic errors which may be introduced by neglecting the wind-tunnel corrections, the test data are subject to random errors of measurement. An estimate of the maximum inaccuracies due to limitations in the balance and recording equipment and the average repeatability of the data indicate that the precision of the drag coefficients is approximately ±0.0003.

RESULTS AND DISCUSSION

Effect of Moment-of-Area-Rule Modifications

The zero-lift drag coefficients of the moment-of-area-rule configurations, the basic wing-body combinations, and the basic body alone are shown plotted versus Mach number in figure 5. The data for the basic wing-body combinations were taken from reference 3. Compared to the

basic wing-body combinations, the moment-of-area-rule configurations had lower drags at transonic speeds and higher drag-divergence Mach numbers; however, at subsonic speeds and also at the higher supersonic Mach numbers, the moment-of-area-rule modifications resulted in increased drag. The maximum reduction in drag coefficient resulting from the moment-of-area-rule modifications was greater and extended over a greater Mach number range for the unswept plan form than for the sweptback or triangular plan forms. On a percentage basis, the moment-of-area-rule configurations with unswept, sweptback, and triangular plan-form wings had maximum drag reductions of approximately 18, 12, and 13 percent, respectively. It should be pointed out that the percentage reductions obtained near Mach number 1.0 would be considerably less if the moment-of-area-rule configurations were compared with transonic-area-rule configurations instead of the basic wing-body combinations.

Because of the additional surface area of the wing-mounted pods, the moment-of-area-rule configurations would be expected to have increased skin friction at all Mach numbers. This increase in friction drag accounts for the higher drag of the moment-of-area-rule configurations at subsonic speeds. At a Reynolds number representative of a full-scale airplane (e.g., Reynolds number of 30 million), the increased friction drag for the moment-of-area-rule configurations at subsonic speeds would be expected to be less than that indicated by these wind-tunnel tests.

The variation of wave drag with Mach number for the moment-of-area rule configurations, the basic wing-body combinations, and the basic body alone is shown in figure 6. Wave drag was obtained by subtracting the friction drag from the total foredrag. In computing the friction drags, it was assumed that at a Mach number of 0.6 the measured drag was entirely due to skin friction and that the variation of friction drag with Mach number was that given by reference 6 for a turbulent boundary layer. As in the case for the total drag, the moment-of-area-rule modifications resulted in lower wave-drag coefficients for all three plan forms at transonic speeds with the largest reduction being obtained with the unswept-wing configuration. It should be noted that since both the moment-of-area rule and the transonic area rule result in the same distribution of cross-sectional area, both rules should give the same wave drag at Mach number 1.0, providing the aspect ratio, wing thickness, and plan form are such that the transonic area rule is applicable. It is shown in references 7 and 8 that for the transonic area rule to be applicable the value of the parameter $A\tau^{1/3}$ should be less than 1.0 for rectangular wings and less than 1.3 for triangular wings. The three wings of the present investigation have a value of $A\tau^{1/3}$ of 0.93. It may be reasoned that area-rule body indentations for higher aspect-ratio wings would lose their effectiveness because the indentations are so far removed from the outer portions of the wing. A moment-of-area-rule design, on the other hand, has indentations in the wing pods as well as in the body and the distances between the indentations and the wing extremities are thus not as great. Experimental evidence of this advantage

[redacted]

of the moment-of-area rule is shown in reference 4 where lower drag was obtained for a supersonic-area-rule design ($A_T^{1/3} = 1.08$) by indenting the engine nacelles as well as the body.

Another manner of presenting the wave-drag data, as recommended in reference 1, is shown in figure 7 in which incremental wave-drag coefficients for the moment-of-area-rule and the basic wing-body configurations were obtained by subtracting the wave drag of the basic body from that of the complete configurations. In contrast to the increases in incremental wave drag displayed (fig. 7) at the higher test Mach numbers by the moment-of-area-rule configurations with unswept, sweptback, and triangular plan-form wings of aspect ratio 3, the results of reference 1 show that a moment-of-area-rule configuration with an elliptic plan-form wing of aspect ratio 2 had lower incremental wave drag at all Mach numbers up to 1.4. It can be established from the theory of reference 1 that because of the increased aspect ratio of the test wings it would be more equitable to compare the effects of the moment-of-area-rule modifications on a reduced aspect ratio basis. In figure 8, the reduction in incremental wave drag (in percent of the maximum possible reduction) predicted by the moment-of-area rule is plotted versus βA for the three plan forms of this investigation as well as for the aspect-ratio-2 elliptic plan-form wing of reference 1. These percentages are subject to a maximum error of ±6 percent because of the inaccuracies in measuring total drag. It may be seen from figure 8, that at the higher values of βA the elliptic plan-form wing of reference 1 would probably have had an increase in incremental wave drag as do the three plan forms of this investigation. Although it would appear from figure 8 that the moment-of-area rule is not effective at the higher values of βA, it should be remembered that these data represent moment-of-area-rule designs for which the distributions of only the area and the second moment of area were made an optimum. The theory of reference 1 indicates that drag reductions can be extended to higher values of βA by taking into account the higher order moments of area. In order to account for these higher order moments, it is necessary to make use of a greater number of auxiliary pods.

Effect of Missile Installations

The second phase of this investigation was concerned with the utilization of the moment-of-area-rule wing pods as supports for carrying four air-to-air type missiles. The total drag coefficients for these configurations are shown in figure 9. For comparison, the drag coefficients of the conventional under-the-wing missile installations and the moment-of-area-rule missile installations which were reported in reference 3 are also shown. Although the configurations of reference 3 utilized the same basic wings, bodies, and missiles as the present investigation, the moment-of-area-rule configurations differed in several ways which would affect their relative drag levels. The moment-of-area-rule

configurations of reference 3 had more optimum distributions of the second moment of area because the missiles were included in the design. On the other hand, the moment-of-area-rule configurations of reference 3 had greater total volume because gloves were added to the sides of the bodies to obtain smooth distributions of area instead of indenting the bodies symmetrically as was done for the present tests. Figure 9 shows that for all three plan forms the drag of the present moment-of-area-rule configurations with missiles was less than the drag of either the conventional missile installation or the moment-of-area-rule missile installation of reference 3.

Figure 10 shows the wave drags of the configurations discussed above. It may be seen that the present moment-of-area-rule configurations with missiles not only had less wave drag than the other configurations with missiles but also had less wave drag than the basic wing-body combination without missiles over part of the transonic speed range. It should be pointed out that the reductions shown would be considerably less if the comparisons were made with transonic area-rule configurations instead of the unmodified wing-body combinations.

For most conventional missile installations, the additional wave drag due to the addition of the missiles is much greater than would be indicated by the wave drag of an isolated missile. These large installation drags are caused by the detrimental interference effects between the missiles themselves and between the missiles and other components of the configuration. The installation wave drags for the configurations of this investigation and those of reference 3 are shown in figure 11. For comparison, a curve representing four times the wave drag of an isolated missile is also shown. It may be seen that the installation wave drags for the moment-of-area-rule configurations of the present investigation were generally less than the wave drag of four isolated missiles; whereas, for the conventional type of installation, the drag due to the addition of the missiles was approximately twice that of four isolated missiles. These results indicate that the interference effect was favorable when the missiles were carried on the moment-of-area-rule pods and unfavorable when the missiles were carried in the conventional manner.

From the foregoing results on the missile installation phase of this investigation, it is apparent that the configurations with moment-of-area-rule pods offer an advantageous means of carrying air-to-air type missiles since such configurations had relatively low drag with or without the missiles in place.

CONCLUDING REMARKS

The effectiveness of the moment-of-area rule when applied to wing-body combinations with unswept, sweptback, and triangular plan-form wings

of aspect ratio 3 has been demonstrated by the results of this investigation. Although the zero-lift drag was reduced a greater amount for the configuration with the unswept wing than it was for the configurations with sweptback or triangular wings, on a percentage basis all three plan forms had approximately 15 percent less total drag than the corresponding unmodified configuration at a Mach number of 1.0. However, at subsonic speeds and at the higher supersonic speeds the modifications resulted in drag penalties.

The results of the tests with four air-to-air type missiles mounted on the pods of the moment-of-area-rule configurations indicate that the pods provided an attractive means of carrying external stores of this type. The moment-of-area-rule models had relatively low drag either with or without the missiles installed. The additional wave drag due to the addition of four missiles to these configurations was in most cases less than four times the drag of an isolated missile; whereas, for the conventional under-the-wing type of installation, the drag due to the addition of the missiles was approximately twice that of four isolated missiles.

Ames Aeronautical Laboratory
National Advisory Committee for Aeronautics
Moffett Field, Calif., Jan. 31, 1958

REFERENCES

1. Baldwin, Barrett S., and Dickey, Robert R.: Application of Wing-Body Theory to Drag Reduction at Low Supersonic Speeds. NACA RM A54J19, 1955.

2. Whitcomb, Richard T.: A Study of the Zero-Lift Drag-Rise Characteristics of Wing-Body Combinations Near the Speed of Sound. NACA RM L52H08, 1952.

3. Levy, Lionel L., and Dickey, Robert R.: External-Store Drag Reduction at Transonic and Low Supersonic Mach Numbers by Application of Baldwin's Moment-of-Area Rule. NACA RM A55L14a, 1956.

4. Hoffman, Sherwood: Supersonic-Area-Rule Design and Rocket-Propelled Flight Investigation of a Zero-Lift Straight-Wing-Body-Nacelle Configuration Between Mach Numbers 0.8 and 1.53. NACA RM L56B27, 1956.

5. Spiegel, Joseph M., and Lawrence, Leslie F.: A Description of the Ames 2- by 2-Foot Transonic Wind Tunnel and Preliminary Evaluation of Wall Interference. NACA RM A55I21, 1955.

[redacted]

6. Chapman, Dean R., and Kester, Robert H.: Turbulent Boundary-Layer and Skin-Friction Measurements in Axial Flow Along Cylinders at Mach Numbers Between 0.5 and 3.6. NACA TN 3097, 1954.

7. Spreiter, John R.: On the Range of Applicability of the Transonic Area Rule. NACA TN 3673, 1956. (Supersedes NACA RM A54F28)

8. Page, William A.: Experimental Determination of the Range of Applicability of the Transonic Area Rule for Wings of Triangular Plan Form. NACA TN 3872, 1956.

[redacted]

TABLE I.- BODY COORDINATES

Body station, in.	Body radius, in.			
	Basic	With unswept wing	With swept-back wing	With triangular wing
0	0	0	0	0
.5	.139	.142	.142	.142
1.0	.230	.235	.235	.235
1.5	.305	.313	.313	.313
2.0	.371	.380	.380	.380
2.5	.427	.440	.440	.440
3.0	.481	.493	.493	.493
3.5	.527	.541	.541	.541
4.0	.570	.585	.585	.585
4.5	.607	.614	.625	.625
5.0	.642	.627	.658	.660
5.5	.671	.636	.689	.690
6.0	.699	.642	.716	.716
6.5	.721	.648	.740	.741
7.0	.741	.652	.754	.758
7.5	.757	.602	.738	.750
8.0	.771	.580	.713	.730
8.5	.780	.585	.688	.709
9.0	.788	.597	.667	.691
9.5	.792	.615	.654	.675
10.0	.794	.640	.650	.665
10.5	.791	.668	.658	.666
11.0	.786	.702	.675	.670
11.5	.778	.723	.699	.680
12.0	.767	.730	.707	.690
12.5	.753	.735	.695	.692
13.0	.735	.737	.675	.681
13.5	.714	.730	.657	.667
14.0	.690	.707	.644	.652
14.5	.663	.678	.630	.636
15.0	.632	.647	.616	.617
15.5	.597	.612	.597	.595
15.644	.585	.601	.591	.590

[redacted]

TABLE II.- POD COORDINATES

Pod station,[1] in.	Pod radius, in.		
	With unswept wing	With swept-back wing	With triangular wing
-4.80	0	---	---
-4.73	---	0	---
-4.68	---	---	0
-4.50	.065	.047	.030
-4.00	.129	.100	.083
-3.50	.177	.140	.114
-3.00	.216	.156	.132
-2.50	.247	.166	.140
-2.00	.272	.170	.145
-1.50	.280	.170	.144
-1.00	.228	.160	.129
-.50	.125	.122	.094
0	.046	.038	.040
.50	.136	.120	.078
1.00	.207	.184	.148
1.50	.258	.221	.232
2.00	.267	.232	.217
2.50	.248	.211	.196
3.00	.217	.184	.169
3.50	.178	.150	.135
4.00	.129	.105	.094
4.50	.065	.047	.034
4.68	---	---	0
4.73	---	0	---
4.80	0	---	---

[1]Measured from midpoint of pod.

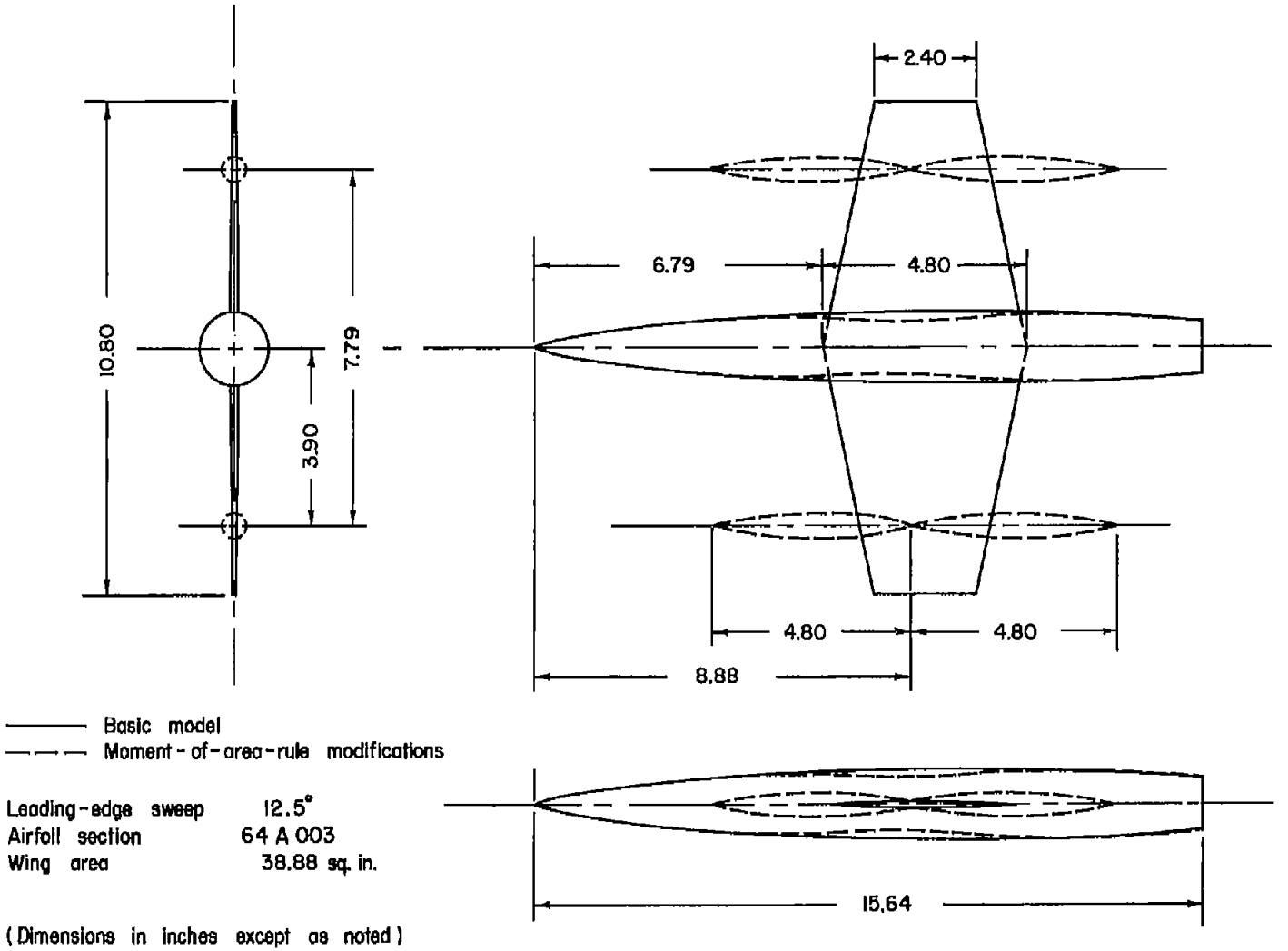

(a) Unswept wing.

Figure 1.- Dimensions of the basic and moment-of-area-rule models.

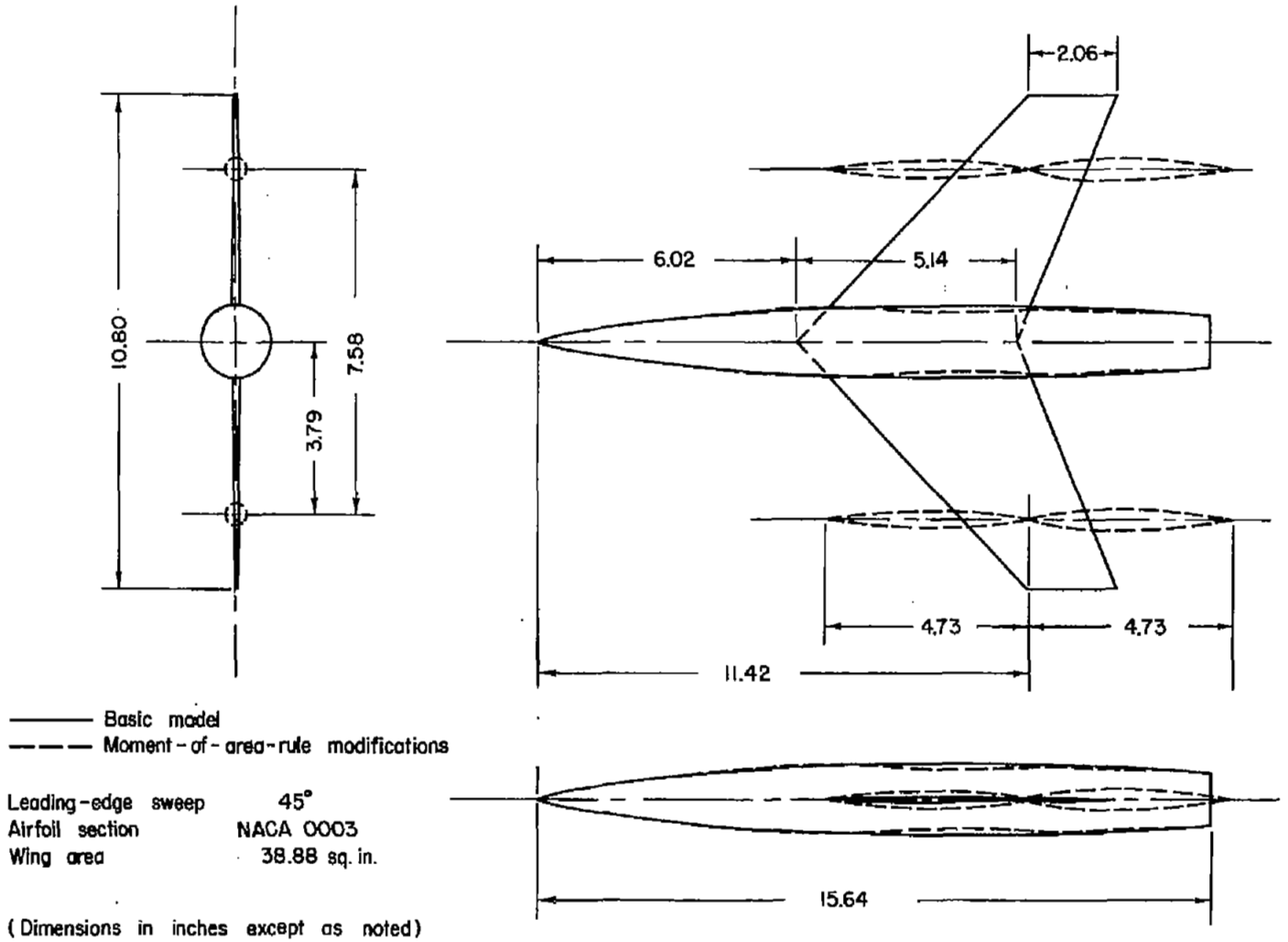

(b) Sweptback wing.

Figure 1.- Continued.

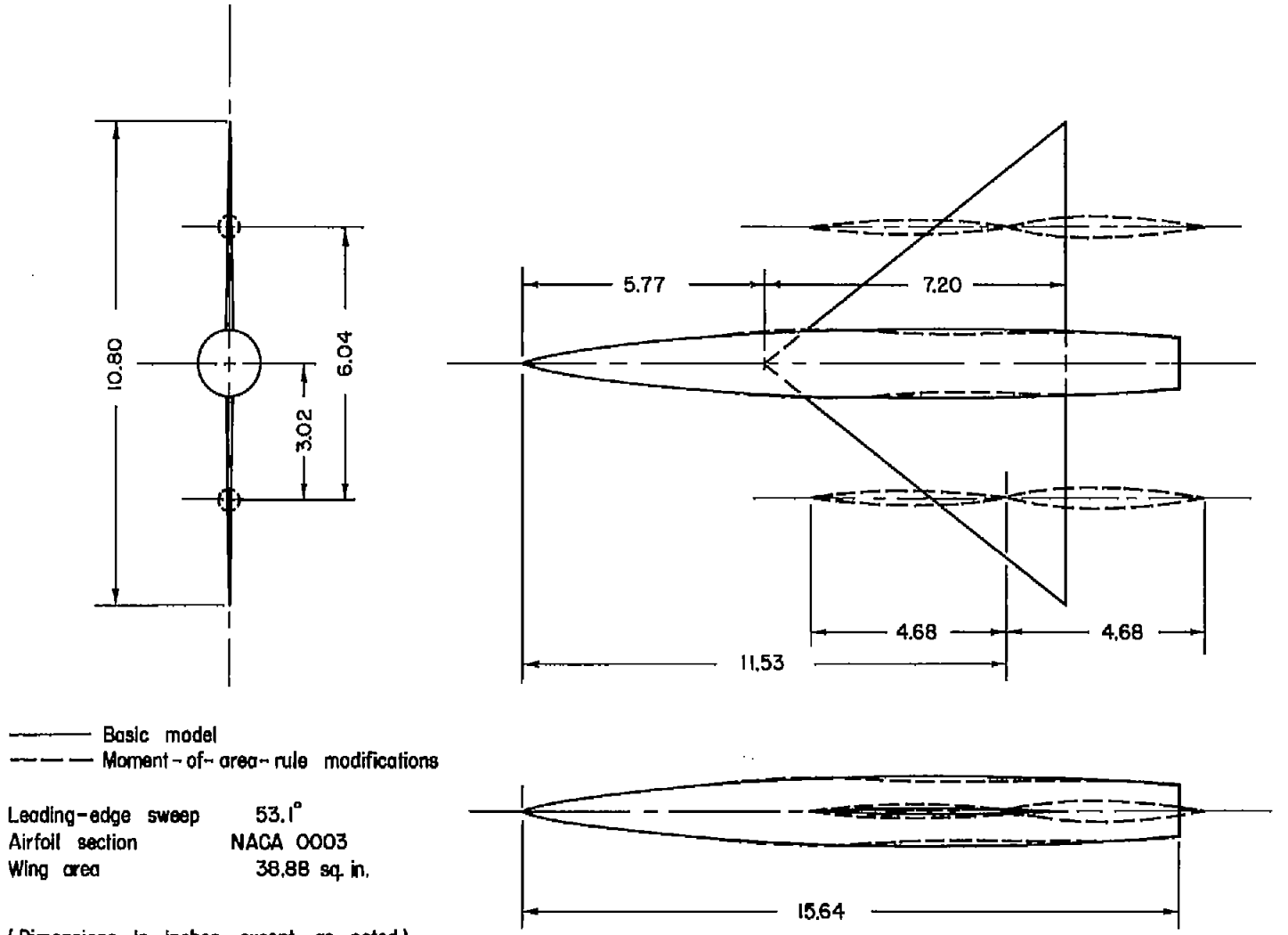

(c) Triangular wing.

Figure 1.- Concluded.

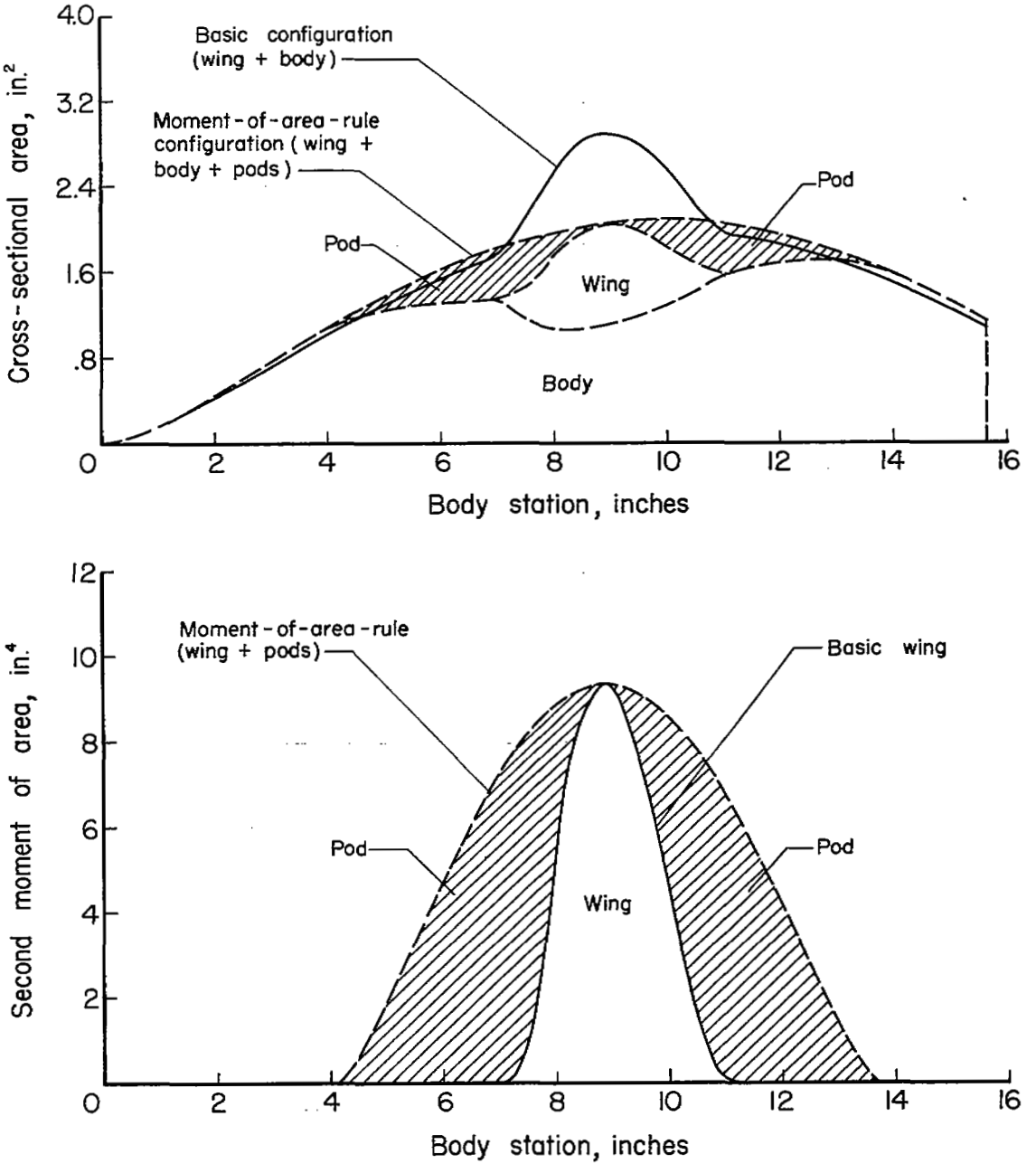

(a) Unswept wing.

Figure 2.- Longitudinal distributions of area and second moment of area for the basic and moment-of-area-rule configurations.

[redacted]

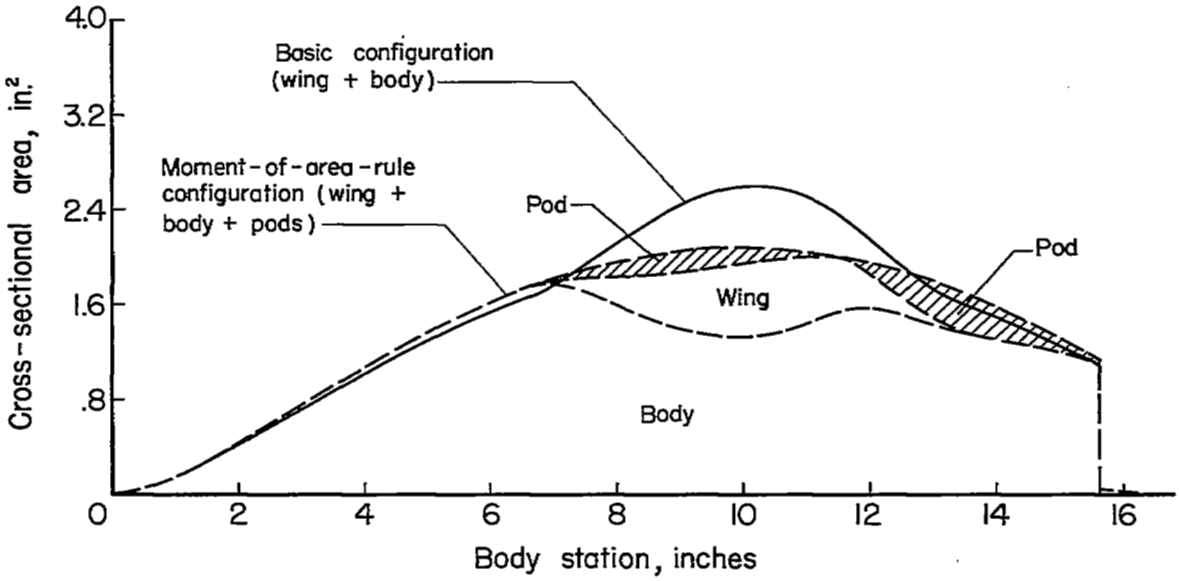

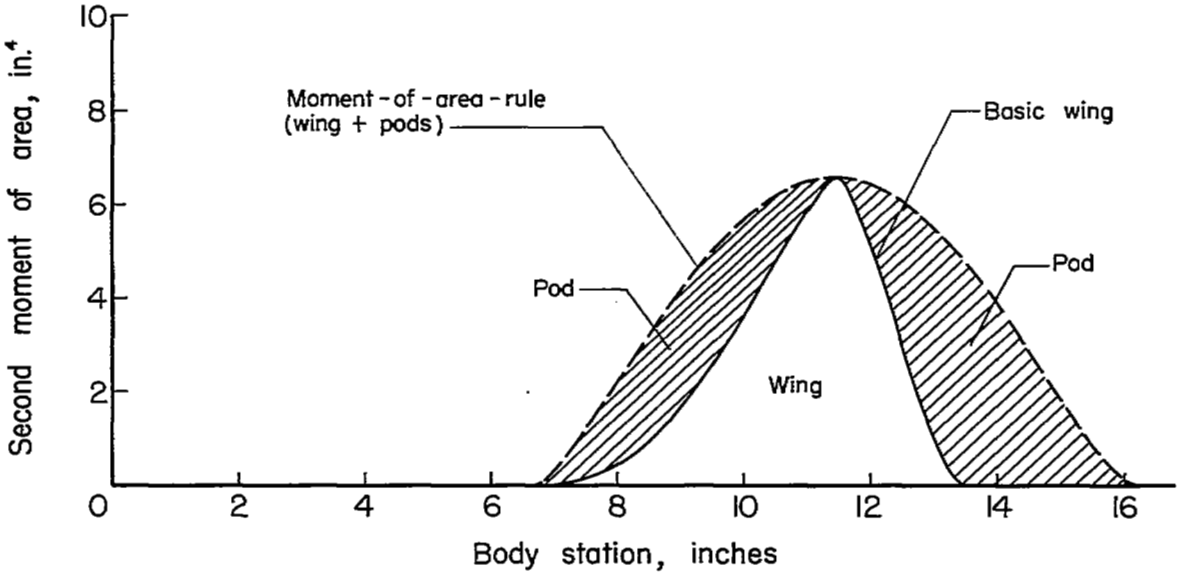

(b) Sweptback wing.

Figure 2.- Continued.

[redacted]

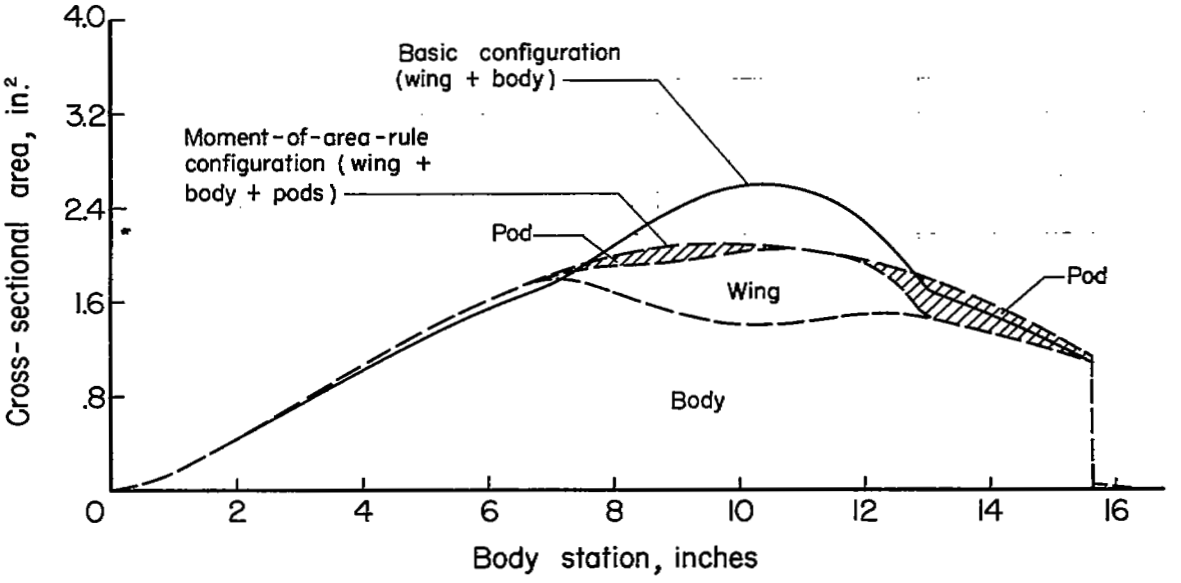

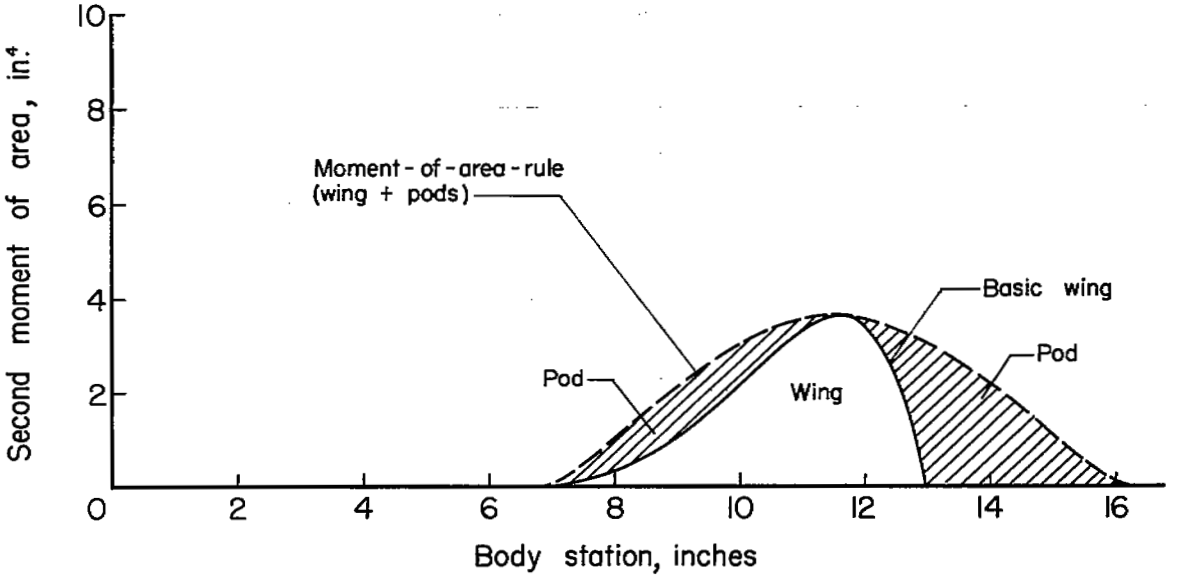

(c) Triangular wing.

Figure 2.- Concluded.

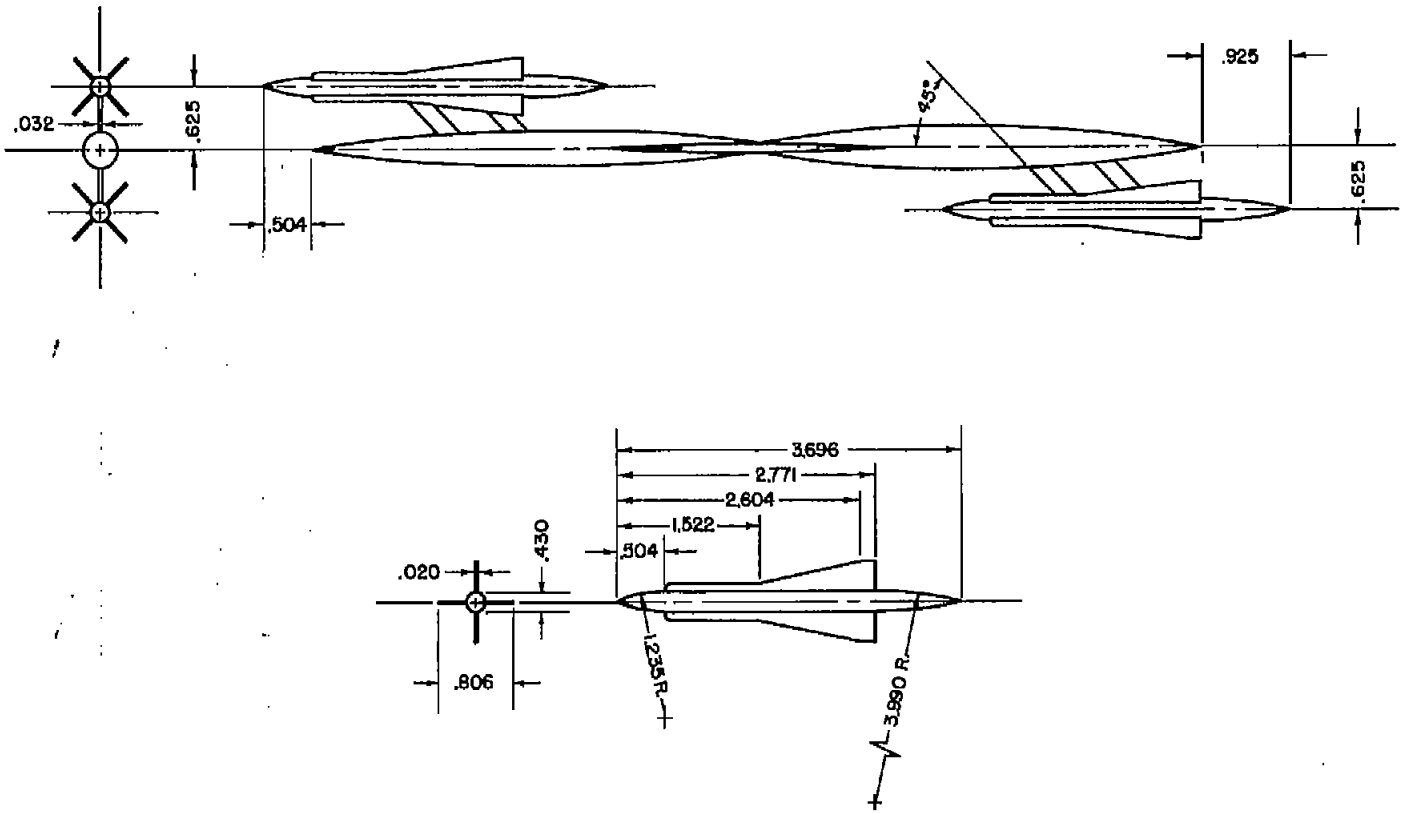

Figure 3.- Typical missile installation.

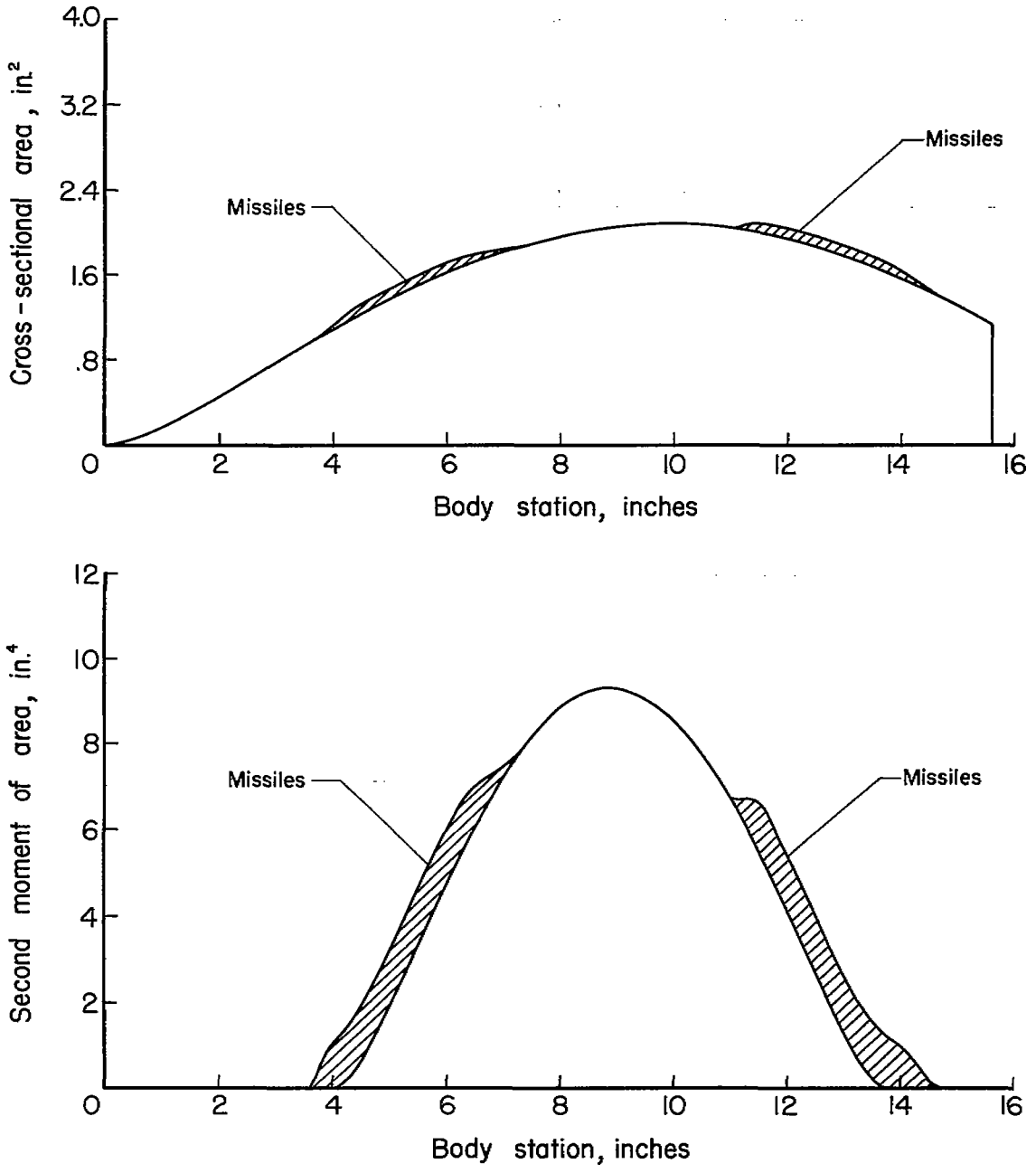

(a) Unswept wing.

Figure 4.- Longitudinal distributions of area and second moment of area for the moment-of-area-rule configurations with missiles.

[redacted]

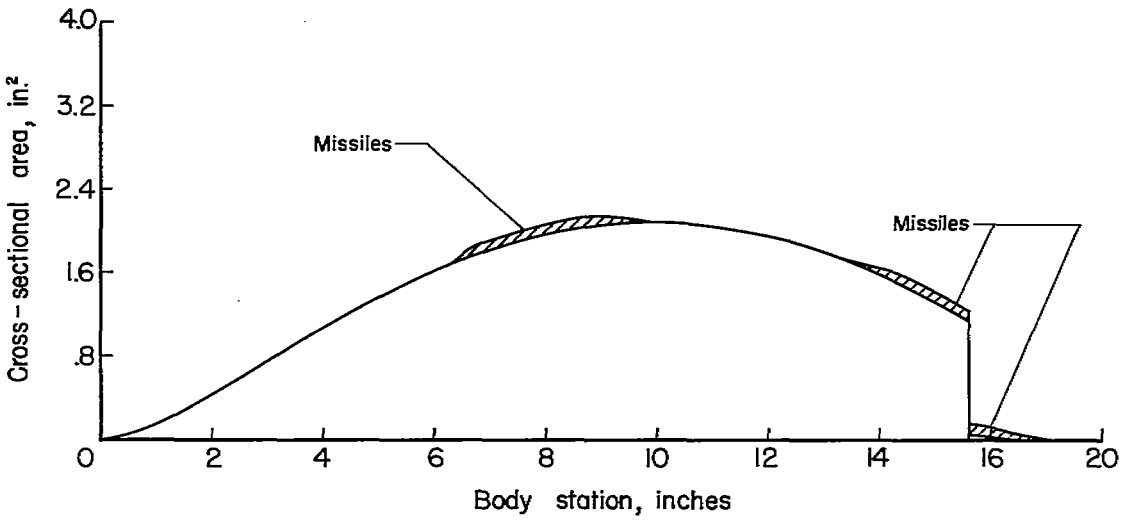

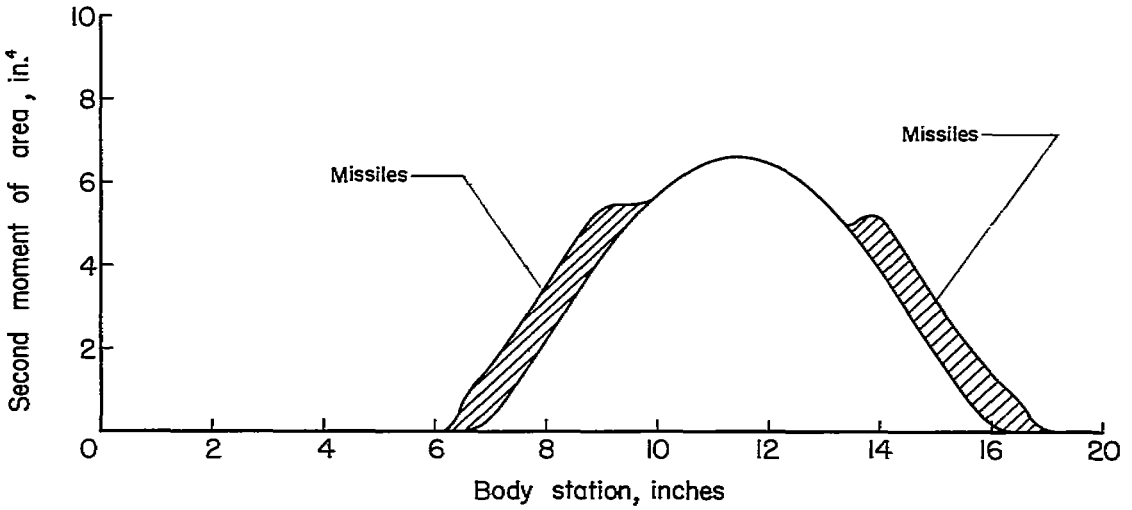

(b) Sweptback wing.

Figure 4.- Continued.

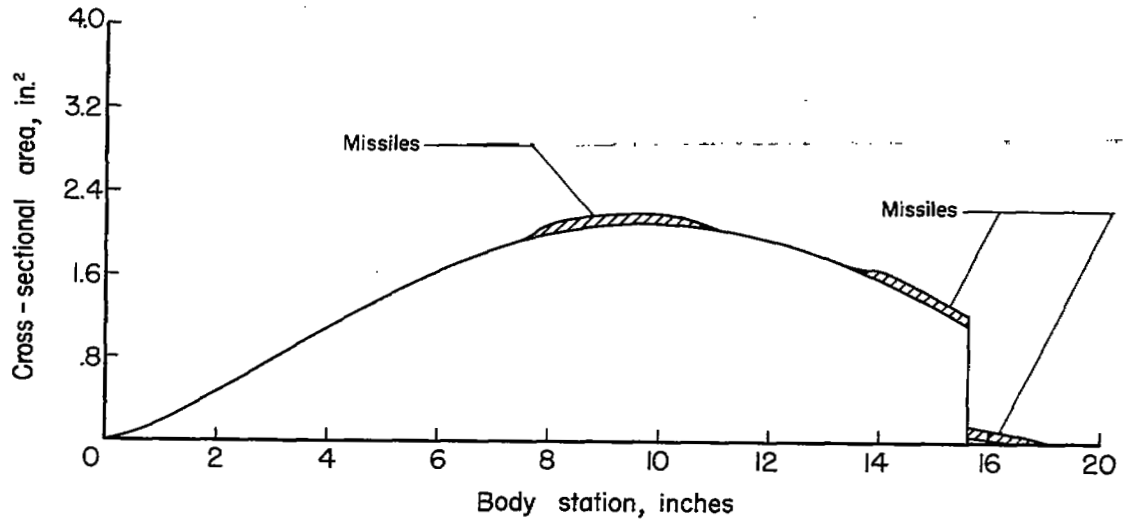

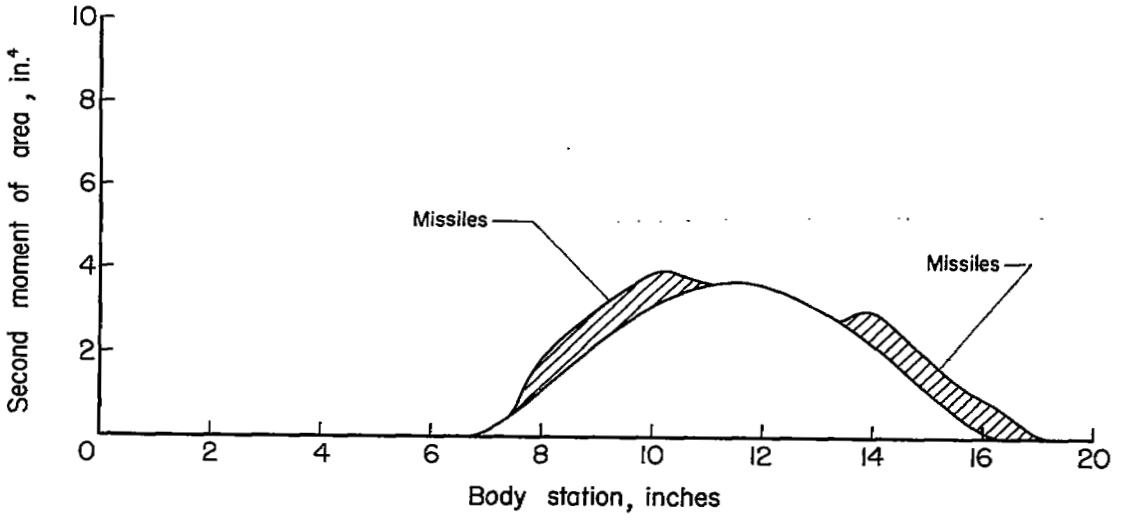

(c) Triangular wing.

Figure 4.- Concluded.

[redacted]

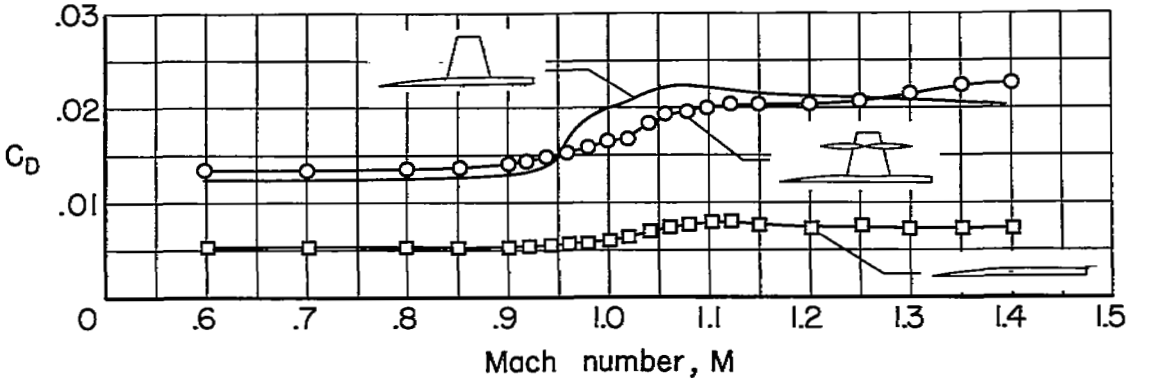

(a) Unswept wing

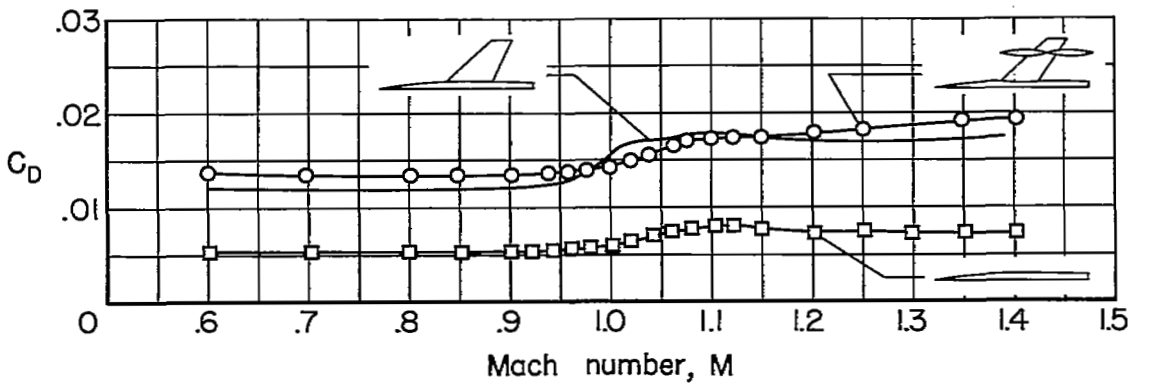

(b) Sweptback wing

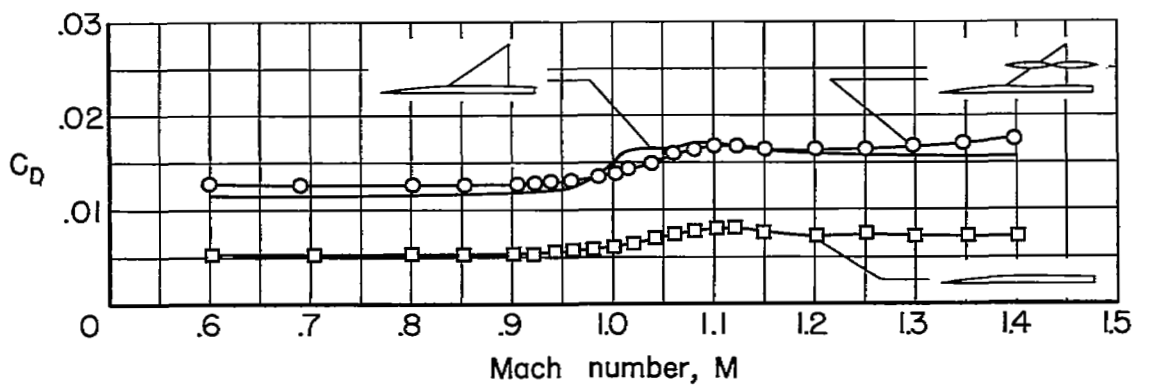

(c) Triangular wing

Figure 5.- Variation of zero-lift drag with Mach number for the basic wing-body combinations, the body alone, and the moment-of-area-rule configurations.

[redacted]

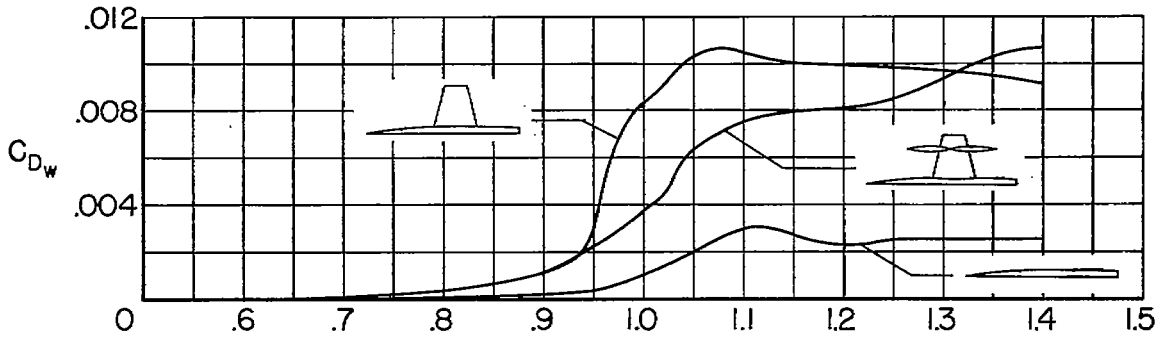

(a) Unswept wing

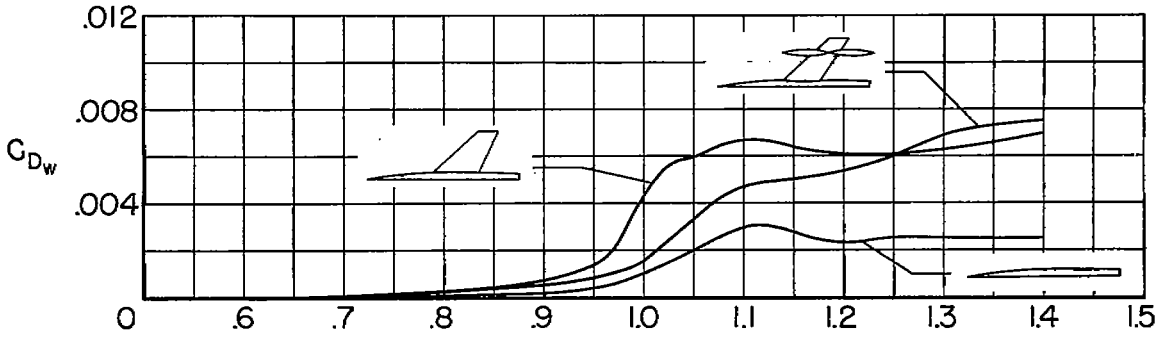

(b) Sweptback wing

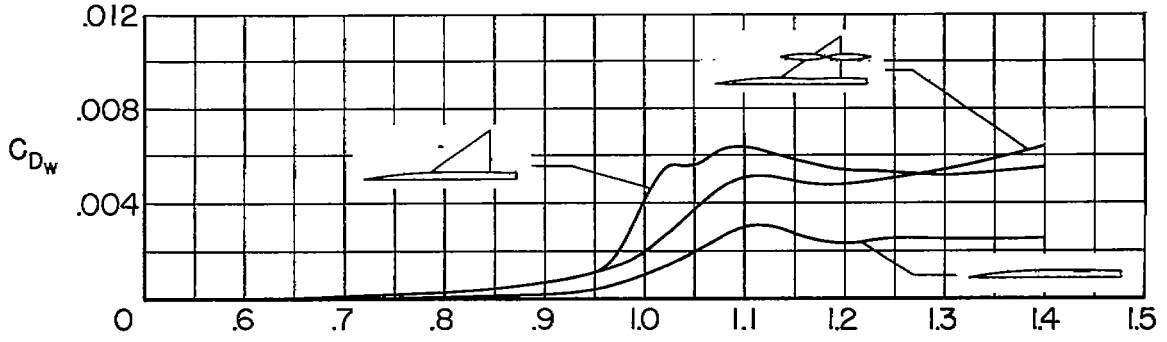

(c) Triangular wing

Figure 6.- Variation of wave drag with Mach number for the basic wing-body combinations, the body alone, and the moment-of-area-rule configurations.

[redacted]

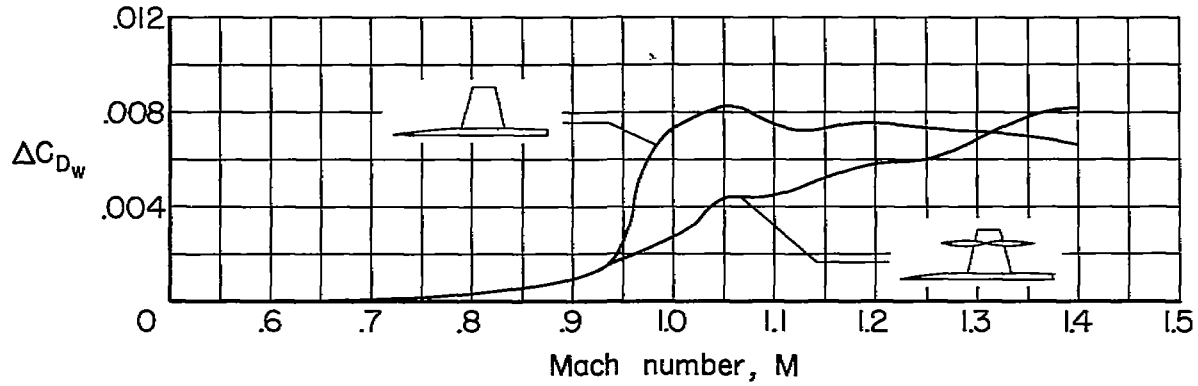

(a) Unswept wing

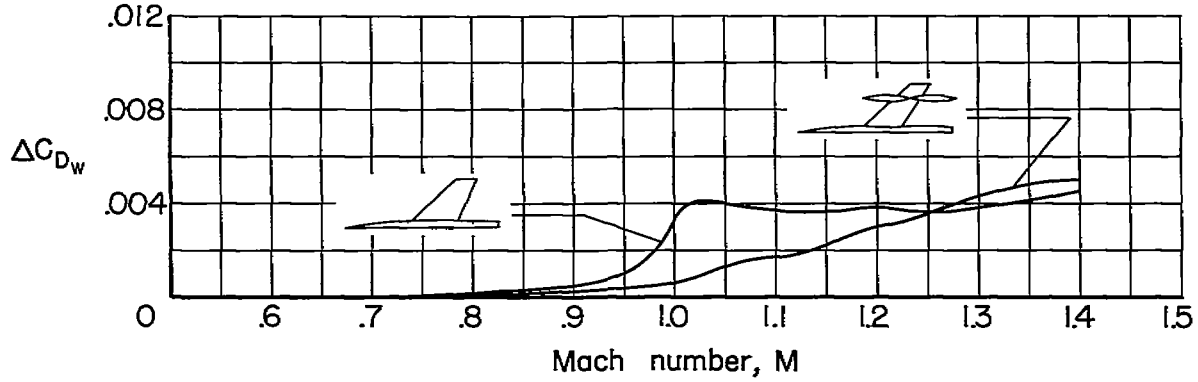

(b) Sweptback wing

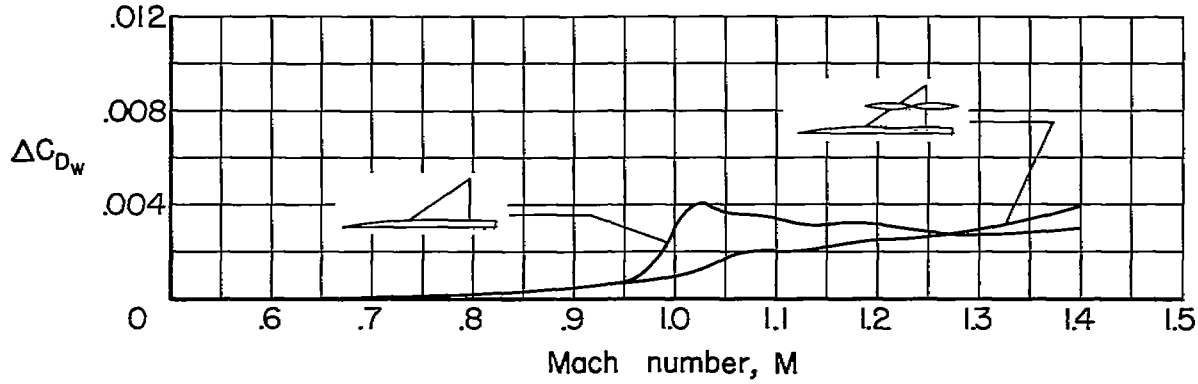

(c) Triangular wing

Figure 7.- Variation of incremental wave drag with Mach number for the basic wing-body combinations and the moment-of-area-rule configurations.

[redacted]

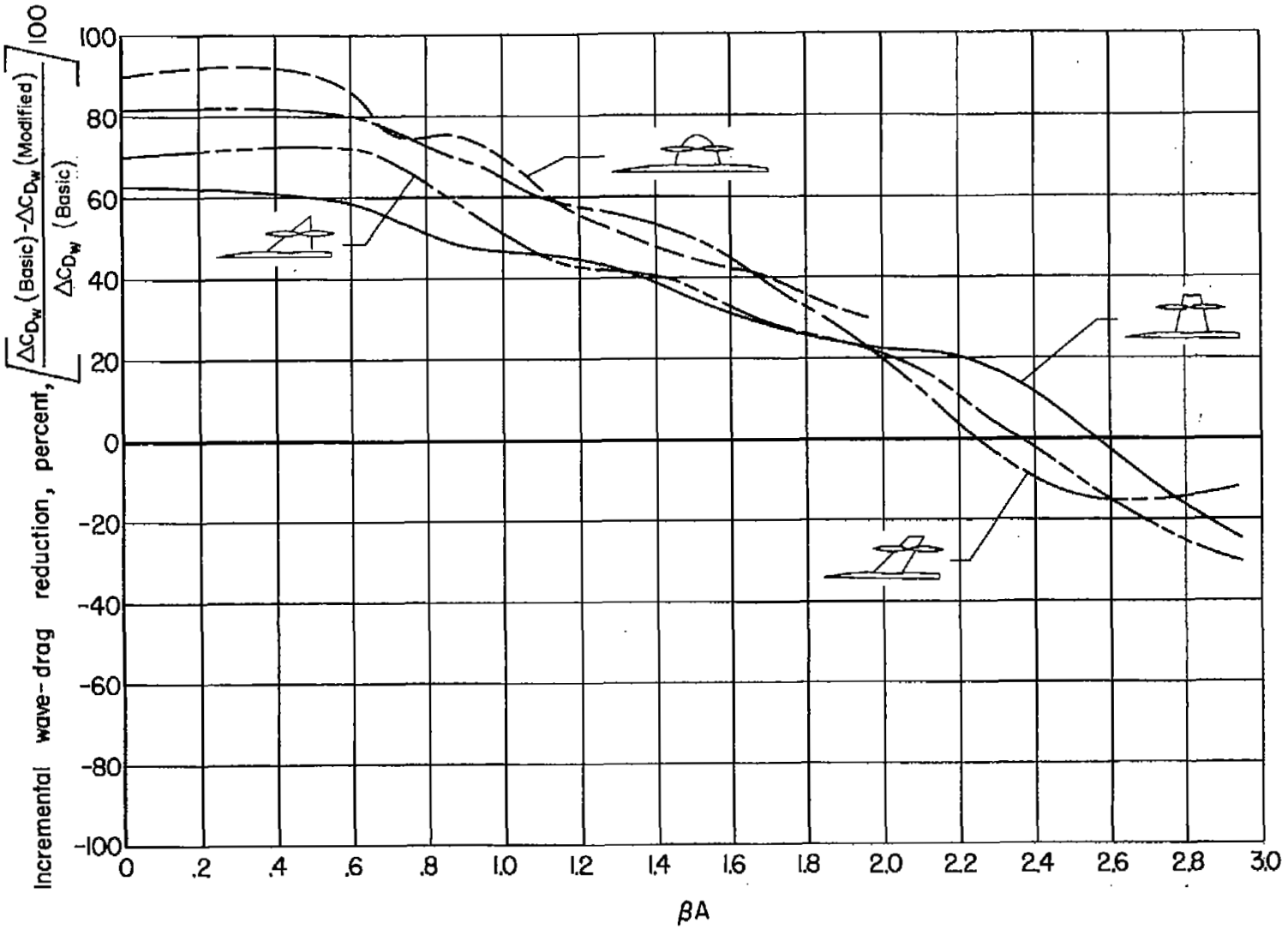

Figure 8.- Variation of incremental wave-drag reduction with reduced aspect ratio.

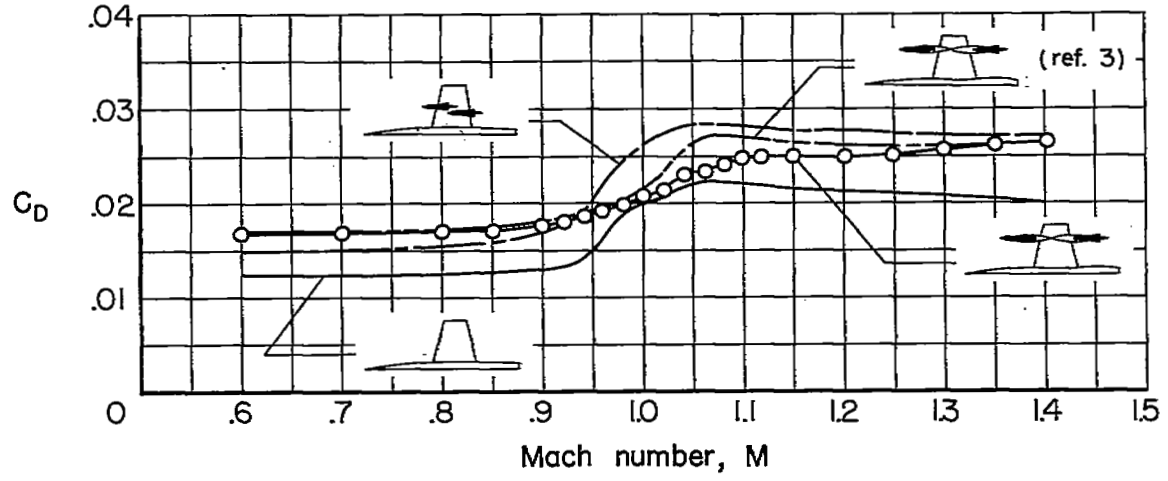

(a) Unswept wing

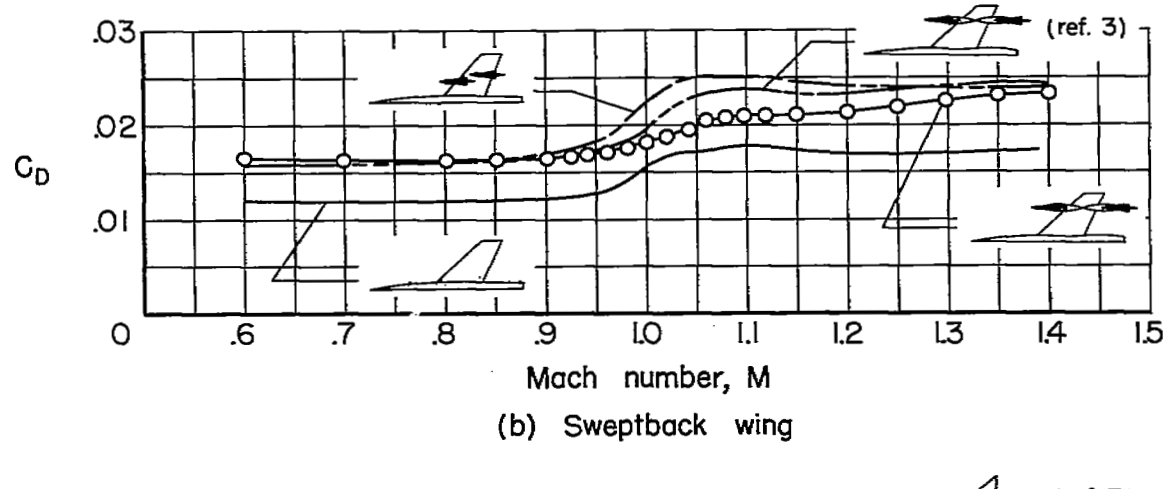

(b) Sweptback wing

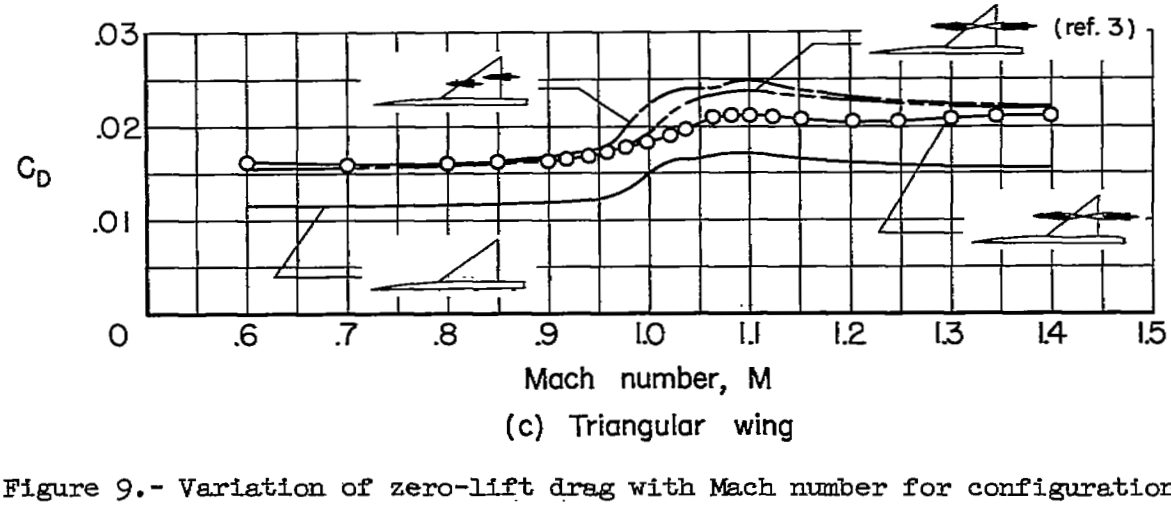

(c) Triangular wing

Figure 9.- Variation of zero-lift drag with Mach number for configurations with missiles.

[redacted]

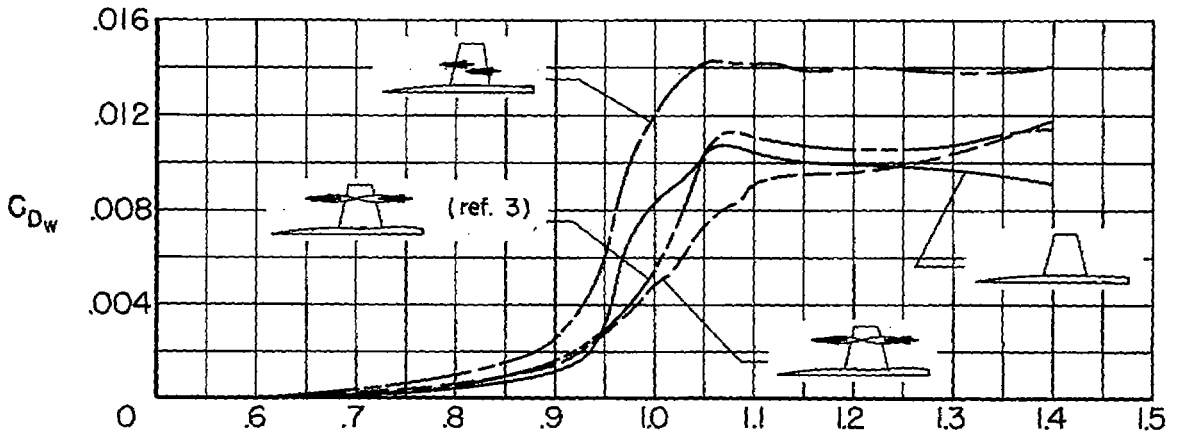

(a) Unswept wing

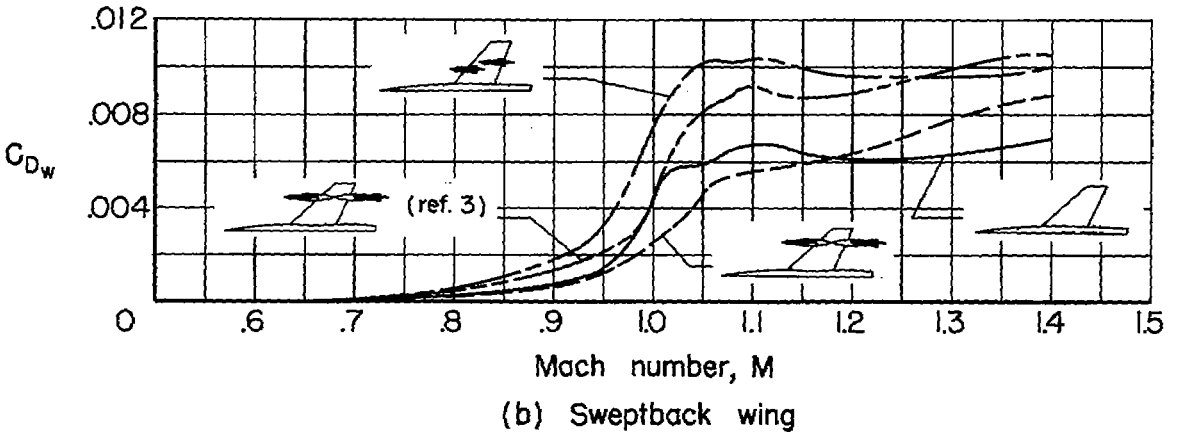

(b) Sweptback wing

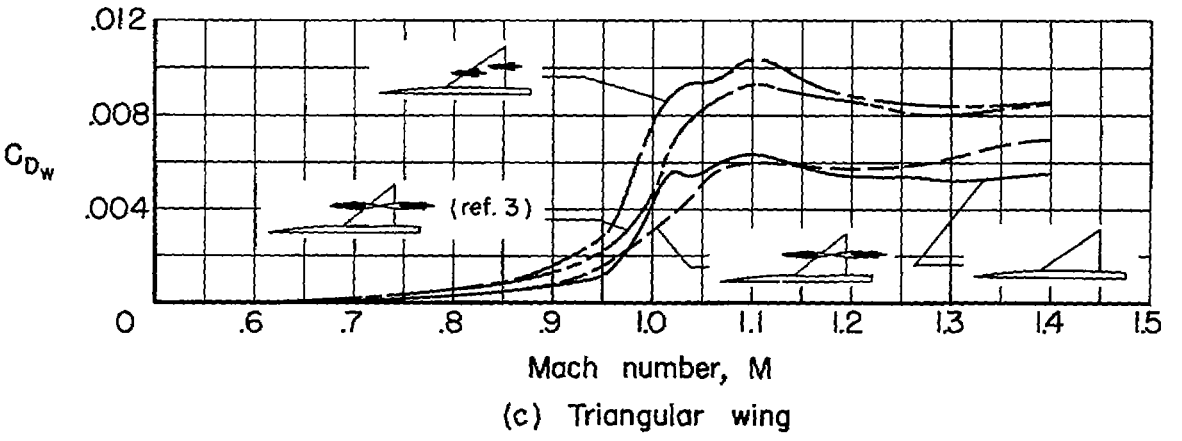

(c) Triangular wing

Figure 10.- Variation of wave drag with Mach number for configurations with missiles.

[redacted]

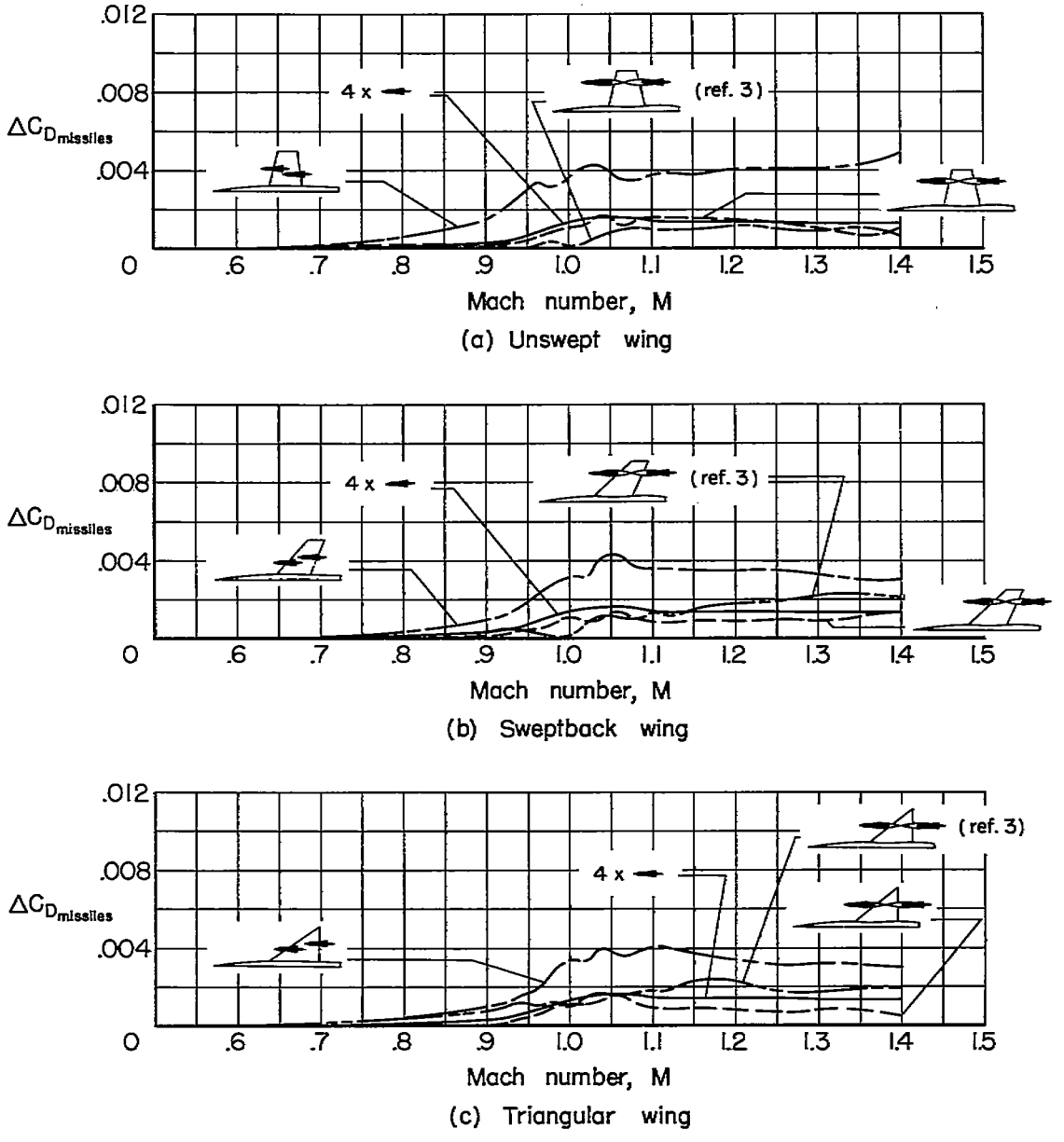

Figure 11.- Variation of missile installation drag with Mach number.

[redacted]